A Study in Photoelectricity

Thesis by

Samuel J. Broadwell

In Partial Fulfillment of the Requirements

for the Degree of Doctor of Philosophy

California Institute of Technology

Pasadena, California

1935

Contents

A Study in Photoelectricity

Summary

A. A theoretical current-voltage relation, for the case of retarding potentials applied to a photoelectric cell, was derived for each of the three cases of plane-parallel, spherical and cylindrical electrodes. When these curves were compared with experimental ones obtained from a sodium cell having spherical electrodes, it was found that the agreement was very poor. The data, treated by the extrapolation method, gave values of Planck's constant in good agreement with that of Birge, thus seeming to show that the theory here developed, rather than the data, is at fault.

B. A test of a new photoelectric effect, described by E. Marx, was investigated and the conclusion reached that no such effect exists in well-constructed cells.

A STUDY OF PHOTOELECTRICITY

The research which forms the subject matter of this thesis was undertaken initially for the purpose of investigating a new photoelectric effect reported by Marx and Meyer. After completion of this study, work was commenced on the problem of an accurate determination of the value of h/e. Since by far the greater part of the work involved was done on this latter problem, the first part of the thesis will be devoted to it, reserving only a few words at the end for the first problem.

Discussion of the Theory of the Photoelectric Determination of h/e.

The ordinary photoelectric determination of Planck's Constant is based upon the theoretical relationship between the maximum kinetic energy of the photoelectrons and the frequency of the incident radiation, as given by the well-known Einstein relation;

$$1/2\ mv^2 = h\nu - b \qquad (1)$$

where the left-hand side of the equation gives the maximum kinetic energy, h is Planck's constant, ν the frequency of the light and b is a constant depending on the work the electron must do in escaping from the electrode. If, now, one electrode of a photoelectric cell be illuminated with monochromatic light of a suitable frequency and the escaping electrons be subjected to a retarding electric field, a current must flow between the electrodes if the retarding field obeys

the inequality;

$$Ve \leq 1/2\ mv^2$$

when V is measured with proper regard for the contact potential. If this limiting potential be measured for a number of different frequencies the two constants of the Einstein equation may be determined.

The proceedure outlined above involves the assumption that a definite maximum electron-emission velocity exists. But this can be true only if the electrons do not share in the thermal motions of the atoms. If they do share the heat energy, then the current-voltage curve must approach the voltage axis asymptotically and there can be no determination of the limiting voltage. A method for overcoming this difficulty, suggested in a paper by Fowler(1) and dealing with the temperature dependence of the photoelectric current, has been developed independently in the Norman Bridge Laboratory and at Washington University by Lee A. DuBridge(2). The method, as developed in these laboratories, will now be given.

Assume the existence, in a metal, of a number of free electrons having thermal energies of agitation distributed in accordance with the Fermi distribution function, and prevented from leaving the metal by a surface potential barrier of height W_a. This is the Sommerfeld picture of the state of the conduction electrons inside a metal. Let the surface of the metal be illuminated by monochromatic light of frequency and assume the probability that a single electron will

absorb a quantum $h\nu$ of energy to be proportional to the component of velocity normal to the surface. Then if the electron is to escape from the metal, the following relation must be true;

$$h\nu + \frac{1}{2} m\xi^2 \geqslant W_a \qquad (2)$$

where ξ is the normal component of velocity inside the metal of the electron. After escaping, the electron can contribute to the current i only if

$$(\frac{1}{2} mv^2)_s \geqslant Ve \qquad (3)$$

where $(\frac{1}{2} mv^2)_s$ signifies the kinetic energy after escape associated with the motion along the lines of force of the field. Since the shape of the field depends on the photoelectric cell used, the discussion will now be limited to the following cases:

A Parallel Plate Electrodes

B Spherical

C Cylindrical

A Parallel Plate Electrodes

In this case the relation between the external field and the energy of the electrons is given by;

$$h\nu + \tfrac{1}{2} m\xi^2 - W_a \geqslant Ve \qquad (4)$$

A consideration of the Fermi distribution of free electrons in momentum space or, since the masses of all electrons will be taken equal,

in velocity space, shows that the electrons are uniformly distributed in a sphere of radius somewhat less than $\sqrt{\frac{2W_i}{m}}$ and having a rapidly decreasing density of distribution outside. The quantity W_i is the maximum energy of an electron at 0° A and is independent of the temperature. Hence at absolute zero the distribution is one of constant electron density inside the sphere and zero density outside.

It is now convenient to refer to a velocity-space diagram in order to see clearly the manner in which the restrictions (2) and (4) limit the photoelectric current. For convenience the sphere of radius $\sqrt{\frac{2W_i}{m}}$ is drawn, although it must be borne in mind that in general the distribution extends to infinity. Now condition (1) restricts the electrons available for the production of the current to those lying above a plane whose equation is;

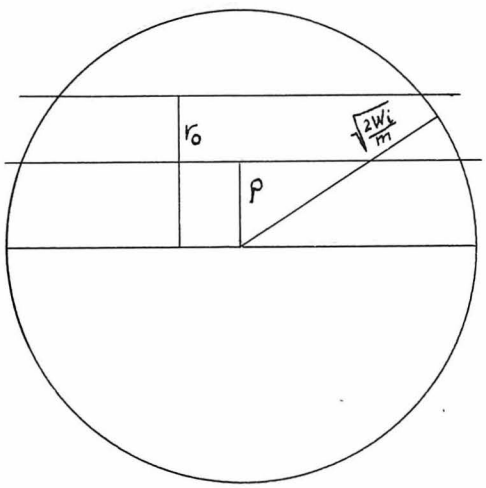

Fig. I

$$\xi = \sqrt{\frac{2}{m}(W_a - h\nu)} = \rho$$

while condition (2) further restricts the number to those lying above a second plane given by;

$$\xi = \sqrt{\frac{2}{m}(W_a - h\nu + Ve)} = v_0$$

Each of the electrons above this second plane has a certain probability of contributing to the current. The current, then, is proportional to the integral, over the space above this second plane, of the electron density multiplied by the probability of ejection; if it is assumed that the probability of transmission through the surface is unity when condition (4) is fulfilled.

The current will then be given by;

$$i = B\int_{cap} \frac{\xi\, d\tau}{Ae^{\frac{\varepsilon}{kT}}+1} \qquad (5)$$

where the integral is to be extended over the volume above the plane $\xi = r_0$; $A = e^{-\frac{W_i}{kT}}$ and $\varepsilon = \frac{m}{2}(\xi^2+\eta^2+\zeta^2)$ the total energy of the electron since the potential energy is assumed zero. Change now to spherical coordinates with the pole in the direction of ξ and the integral becomes;

$$i = B\int_0^{2\pi}\int_0^{\cos^{-1}\frac{r_0}{r}}\int_{r_0}^{\infty} \frac{r^3\cos\theta\sin\theta\, dr\, d\theta\, d\phi}{Ae^{\frac{mr^2}{2kT}}+1}$$

The integration over ϕ and θ may be carried out immediately, giving

$$i = \pi B\int_{r_0}^{\infty} \frac{r^3 dr}{Ae^{\frac{mr^2}{2kT}}+1} - \pi B\int_{r_0}^{\infty} \frac{r_0^2 r\, dr}{Ae^{\frac{mr^2}{2kT}}+1}$$

These integrals cannot be evaluated in closed form and the expansions involved are valid either for $r<\sqrt{\frac{2W_i}{m}}$ or $r>\sqrt{\frac{2W_i}{m}}$; hence an expression for i must be obtained in each of these regions. Upon carrying out the necessary steps, the following expressions are obtained for the current:

Region 1 $r_0 \leq \sqrt{\frac{2W_i}{m}}$

$$i = 2\left(\frac{KT}{m}\right)^2 \pi B\left[\frac{\pi^2}{6} + \frac{1}{2}\gamma^2 - (e^{\gamma} - \frac{1}{2^2}e^{2\gamma} + \frac{1}{3^2}e^{3\gamma} - \cdots)\right] \quad (6)$$

Region 2 $r_0 \geq \sqrt{\frac{2W_i}{m}}$

$$i = 2\left(\frac{KT}{m}\right)^2 \pi B\left[e^{-\gamma} - \frac{1}{2^2}e^{-2\gamma} + \frac{1}{3^2}e^{-3\gamma} - \cdots\right] \quad (7)$$

where $\gamma = \frac{W_a - W_i - h\nu + Ve}{KT} = \frac{mr_0^2}{2KT} - \frac{W_i}{KT}$

It is seen that when $r_0 = \sqrt{\frac{2W_i}{m}}$, $\gamma = 0$; therefore for region 1

$$\gamma \leq 0$$

while for region 2

$$\gamma \geq 0$$

But when $\gamma = 0$, $W_a - W_i - h\nu + Ve = 0$, or since W_a and W_i are constants depending on the metal, $W_a - W_i = b$, and

$$Ve = h\nu - b$$

It is interesting to note that the value of the current given by equations (6) and (7) is greater than zero for $\gamma = 0$ and that the current becomes zero only for $\gamma = \infty$. This is in disagreement with the usual experimental method of extrapolating the current-voltage curve to zero current and inserting the so-obtained voltage value into the Einstein equation. It appears from this analysis that the current-voltage curve approaches the voltage axis aymptotically and that there is no purely experimental method of determining the

point on the curve for which Einstein's equation holds. Only at $0^{o}A$, as may readily be seen by inspection of equations (6) and (7), does the current go to zero for $\gamma=0$.

Expressions for the photocurrent in the plane-parallel case have been given by Fowler[1] and DuBridge[2]. The assumptions underlying them are identical with those of the present paper with the one exception that they used a constant value for the excitation probability. Fowler plotted the current as a function of the frequency and worked near the threshold, while DuBridge plotted current against voltage and found experimental agreement for the region of currents near the stopping potential, but not in that of saturation currents. He ascribes the failure in this region to reflected electrons.

The DuBridge and Fowler expressions, which for this case are identical, are given below, where the notations have been changed to conform with the present paper.

$$i = const\,(KT)^{3/2}\left(\gamma-\frac{W_i}{KT}\right)^{1/2}\left[\frac{\pi^2}{6}+\frac{\gamma^2}{2}-\left(e^{\gamma}-\frac{1}{2^2}e^{2\gamma}+\frac{1}{3^2}e^{3\gamma}-\cdots\right)\right] \quad \text{for } \gamma\leq 0$$

$$i = const\,(KT)^{3/2}\left(\gamma-\frac{W_i}{KT}\right)^{1/2}\left[e^{-\gamma}-\frac{1}{2^2}e^{-2\gamma}+\frac{1}{3^2}e^{-3\gamma}-\cdots\right] \quad \text{for } \gamma\geq 0$$

It is seen that these expressions are the same, except for the factor $\left(\gamma-\frac{W_i}{KT}\right)^{1/2}$ with the just derived equations (6) and (7). The significant feature is that the current is a function of a single variable γ . Hence, the current-voltage curves should have the same form for all frequencies.

Case B. Spherical Electrodes.

The assumption given in equation 2 will hold for the case of a spherical emitting surface, as well as for a plane, since the distance travelled by an electron in leaving the surface is infinitesimal in comparison with the radius of curvature of the surface. However equation (4) must now be replaced by;

$$h\nu + \tfrac{1}{2} m(\xi^2 + \eta^2 + \zeta^2) - W_a \geq V_e \qquad (8)$$

Hence the integration will be over that part of the phase-space lying above the plane ρ and outside the sphere r_0 of Fig. 2. The expression for the current then becomes;

$$i = B \int_0^{2\pi} \int_0^{\cos^{-1}\frac{\rho}{r}} \int_{r_0}^{\infty} \frac{r^3 \cos\theta \sin\theta \, dr \, d\theta \, d\phi}{A e^{\frac{mr^2}{2kT}} + 1}$$

where, as before;

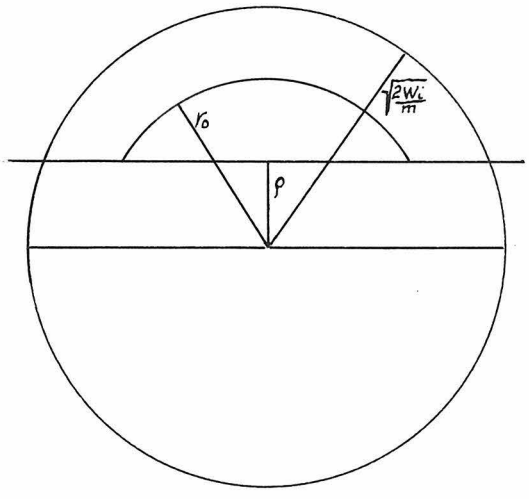

Fig II

$$\rho = \sqrt{\frac{2}{m}(W_a - h\nu)}$$

$$r_0 = \sqrt{\frac{2}{m}(W_a - h\nu + V_e)}$$

$$r = \sqrt{(\xi^2 + \eta^2 + \zeta^2)}$$

Here also the integration over the angle variables may be carried out directly, giving;

$$i = \pi B \int_{r_0}^{\infty} \left(1 - \frac{\rho^2}{r^2}\right) \frac{r^3 dr}{A e^{\frac{mr^2}{2kT}} + 1}$$

$$= \pi B \int_{r_0}^{\infty} \frac{r^3 dr}{A e^{\frac{mr^2}{2kT}} + 1} - \pi B \rho^2 \int_{r_0}^{\infty} \frac{r dr}{A e^{\frac{mr^2}{2kT}} + 1}$$

Upon making the following substitutions,

$$\frac{mr^2}{2KT} = \log x$$

$$\frac{W_i}{KT} = \alpha = -\log A$$

$$X_0 = e^{\gamma+\alpha}$$

the expression for the current becomes;

$$i = 2\pi B\left(\frac{KT}{m}\right)^2\left[\int_{e^{\gamma+\alpha}}^{\infty} \frac{\log x\,dx}{X(AX+1)} - \frac{W_a - h\nu}{KT}\int_{e^{\gamma+\alpha}}^{\infty} \frac{dx}{X(AX+1)}\right.$$

which may be further simplified to;

$$i = 2\pi B\left(\frac{KT}{m}\right)^2\left[\int_{e^{\gamma+\alpha}}^{\infty} \frac{\log x\,dx}{X} - \int_{e^{\gamma+\alpha}}^{\infty} \frac{A\log x\,dx}{AX+1} - \frac{W_a - h\nu}{KT}\int_{e^{\gamma+\alpha}}^{\infty} \frac{dx}{X} + \frac{W_a - h\nu}{KT}\int_{e^{\gamma+\alpha}}^{\infty} \frac{dx}{AX+1}\right]$$

The term

$$\int_{e^{\gamma+\alpha}}^{\infty} \frac{A\log x\,dx}{AX+1}$$

may be expanded in series of ascending or descending powers of Ax depending on whether Ax $>$ 1 or $<$ 1. In the region $\gamma < 0$, Ax passes over this critical value, hence for region 1, $\gamma \leq 0$ the current is given by;

$$i = 2\pi B\left(\frac{KT}{m}\right)^2\left[\int_{e^{\gamma+\alpha}}^{\infty} \frac{\log x\,dx}{X} - \int_{e^{\gamma+\alpha}}^{\frac{1}{A}} \frac{A\log x\,dx}{AX+1} - \int_{\frac{1}{A}}^{\infty} \frac{A\log x\,dx}{AX+1} - \frac{W_a - h\nu}{KT}\int_{e^{\gamma+\alpha}}^{\infty} \frac{dx}{X} + \frac{W_a - h\nu}{KT}\int_{e^{\gamma+\alpha}}^{\infty} \frac{A\,dx}{AX+1}\right.$$

while for region 2, $\gamma \geq 0$ Ax is always greater than 1 and a single expansion suffices.

The final expressions for the currents in the two cases are then given by;

Region 1 $\gamma \leq 0$

$$i = 2\pi B\left(\frac{KT}{m}\right)^2\left[\frac{\pi^2}{6} + \frac{1}{2}\gamma^2 + (\gamma-\sigma)\log(e^{-\gamma}+1) - \left(e^{\gamma} - \frac{1}{2^2}e^{2\gamma} + \frac{1}{3^2}e^{3\gamma} - \cdots\right)\right] \qquad (9)$$

Region 2 $\gamma \geq 0$

$$i = 2\pi B\left(\frac{KT}{m}\right)^2\left[(\gamma-\sigma)\log(e^{-\gamma}+1) + \left(e^{-\gamma} - \frac{1}{2^2}e^{-2\gamma} + \frac{e^{-3\gamma}}{3^2} - \cdots\right)\right] \qquad (10)$$

where $\sigma = \frac{W_a - W_i - h\nu}{KT}$

Case C. Cylindrical Electrodes.

This case is much more involved than the two preceeding, since the electron distribution possesses spherical symmetry while the electric field is cylindrical. It was not found possible to carry out the integrations in any manner except mechanically.

For the cylindrical case, equation (2) is valid, while the field-limiting equation becomes;

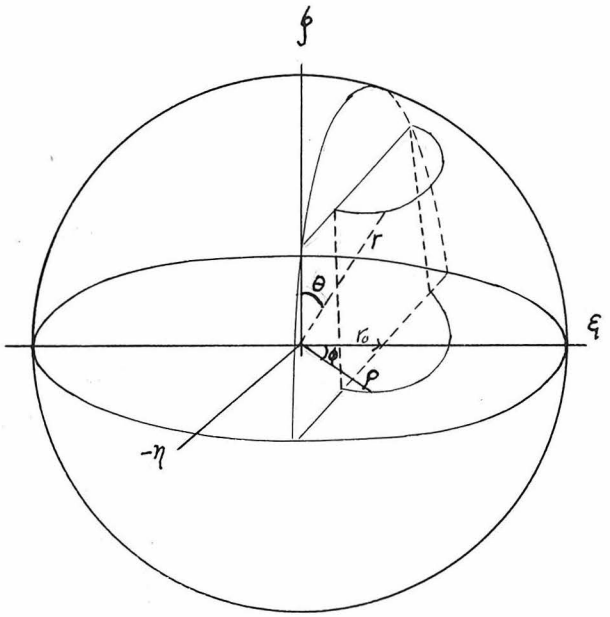

Fig III

$$h\nu + \frac{1}{2}m(\xi^2+\eta^2) - W_a \geq Ve \qquad (11)$$

It is found most convenient to arrange the coordinate system as shown in Figure 3, where the polar axis of the spherical system is parallel to ζ . Then

$$\frac{1}{2}m(\xi^2+\eta^2) = \frac{1}{2}m\rho^2$$

and

$$\frac{1}{2}m(\xi^2+\eta^2+\zeta^2) = \frac{1}{2}mr^2$$

$$W_a - h\nu = \frac{1}{2}mr_o^2$$

The limits in this case become

$$\rho \leq r \leq \infty$$

$$\sin^{-1}\frac{\rho}{r} \leq \theta \leq \frac{\pi}{2}$$

$$0 \leq \phi \leq \cos^{-1}\frac{r_o}{r\sin\theta}$$

The integral for the current becomes on inserting these limits and multiplying by 4 to take into account the symmetrical quadrants excluded by the choice of limits;

$$i = 4B\int_0^{\cos^{-1}\frac{r_o}{r\sin\theta}}\int_{\sin^{-1}\frac{\rho}{r}}^{\frac{\pi}{2}}\int_\rho^\infty \frac{\xi r^2\sin\theta\, dr\,d\theta\,d\phi}{Ae^{\frac{mr^2}{2kT}}+1}$$

or since

$$\xi = r\sin\theta\cos\phi$$

this becomes

$$i = 4B\int_0^{\cos^{-1}\frac{r_o}{r\sin\theta}}\int_{\sin^{-1}\frac{\rho}{r}}^{\frac{\pi}{2}}\int_\rho^\infty \frac{r^3\sin^2\theta\cos\phi\, dr\,d\theta\,d\phi}{Ae^{\frac{mr^2}{2kT}}+1} \qquad (12)$$

Integration over the angle variables yield the result;

$$i = 2B\int_{\rho}^{\infty} \frac{r}{Ae^{\frac{mr^2}{2KT}}+1}\left[\sqrt{r^2-\rho^2}\sqrt{\rho^2-r_0^2} + (r^2-r_0^2)\sin^{-1}\sqrt{\frac{r^2-\rho^2}{r^2-r_0^2}}\right]dr$$

It is convenient to rewrite this expression

$$i = 4B\left(\frac{KT}{m}\right)^2\int_{\gamma+\alpha}^{\infty} \frac{d\gamma}{Ae^{\gamma}+1}\left[\sqrt{\gamma-\gamma-\alpha}\sqrt{\gamma-\sigma} + (\gamma-\beta)\sin^{-1}\sqrt{\frac{\gamma-\gamma-\alpha}{\gamma-\beta}}\right]$$

by means of the following transformations;

$$\gamma = \frac{mr^2}{2KT}$$

$$\gamma+\alpha = \frac{m\rho^2}{2KT}$$

$$\alpha = \frac{W_i}{KT}$$

$$\beta = \frac{mr_0^2}{2KT}$$

$$\gamma-\sigma = \frac{m\rho^2-mr_0^2}{2KT}$$

If this be further changed by the substitution;

$$\gamma-\gamma-\alpha = y$$

the integral finally becomes;

$$i = 4\left(\frac{KT}{m}\right)^2 B\int_0^{\infty} \frac{dy}{e^{\gamma+y}+1}\left[\sqrt{\gamma-\sigma}\sqrt{y} + (\gamma-\sigma+y)\sin^{-1}\sqrt{\frac{y}{\gamma-\sigma+y}}\right] \qquad (13)$$

in which form the integration may be carried out mechanically.

Discussion of Theoretical Curves.

The five expressions 6, 7, 9, 10 and 13 may now be written down for comparison. We have;

Case A. Plane.

$$i = 2\left(\frac{KT}{m}\right)^2 \pi B \left[\frac{\pi^2}{6} + \frac{1}{2}\gamma^2 - (e^{\gamma} - \frac{1}{2^2}e^{2\gamma} + \frac{1}{3^2}e^{3\gamma} - \cdots)\right] \qquad \text{for } \gamma \leq 0$$

$$i = 2\left(\frac{KT}{m}\right)^2 \pi B \left[e^{-\gamma} - \frac{1}{2^2}e^{-2\gamma} + \frac{1}{3^2}e^{-3\gamma} - \cdots\right] \qquad \text{for } \gamma \geq 0$$

Case B. Spherical.

$$i = 2\left(\frac{KT}{m}\right)^2 \pi B \left[\frac{\pi^2}{6} + \frac{1}{2}\gamma^2 + (\gamma - \sigma)\log(e^{-\gamma}+1) - (e^{\gamma} - \frac{1}{2^2}e^{2\gamma} + \frac{1}{3^2}e^{3\gamma} - \cdots)\right] \qquad \text{for } \gamma \leq 0$$

$$i = 2\left(\frac{KT}{m}\right)^2 \pi B \left[(\gamma - \sigma)\log(e^{-\gamma}+1) + (e^{-\gamma} - \frac{1}{2^2}e^{-2\gamma} + \frac{1}{3^2}e^{-3\gamma} - \cdots)\right] \qquad \text{for } \gamma \geq 0$$

Case C. Cylindrical.

$$i = 4\left(\frac{KT}{m}\right)^2 B \int_0^{\infty} \frac{dy}{e^{\gamma+y}+1}\left[\sqrt{\gamma-\sigma}\,\sqrt{y} + \sqrt{\gamma-\sigma+y}\,\sin^{-1}\sqrt{\frac{y}{\gamma-\sigma+y}}\right]$$

As has already been shown, case A yields a function of one variable alone if the temperature be maintained constant. This is no longer true, however, if the photocell has spherical or cylindrical symmetry, for in these cases the constant σ enters, and since this is the difference between the total work-function and the incident quantum, it will be necessary to have a theoretical curve for each separate frequency of light used experimentally.

The proportionality constant B involves the intensity of illumination incident on the photocell. If log i rather than i be plotted as a function of γ, then log B will be an additive constant which will shift the entire curve up or down.

DuBridge has given a theoretical treatment of the spherical

case which yields the expressions;

$$i = AK^2T^2\left\{\frac{\pi^2}{6} - \frac{1}{2}\left[\left(\frac{Ve}{KT}\right)^2 - \sigma^2\right] + \frac{Ve}{KT}\log(1+e^{\gamma}) - (e^{\gamma} - \frac{1}{2^2}e^{2\gamma} + \frac{1}{3^2}e^{3\gamma} - \cdots)\right\} \qquad \text{for } \gamma \leq 0$$

$$i = AK^2T^2\left\{-\frac{Ve}{KT}\gamma + \frac{Ve}{KT}\log(1+e^{\gamma}) + (e^{-\gamma} - \frac{1}{2^2}e^{2\gamma} + \frac{1}{3^2}e^{-3\gamma} - \cdots)\right\} \qquad \text{for } \gamma \geq 0$$

These expressions may be reduced to the equations (9) and (10) here derived, but the method of derivation necessitated the assumptions that the probability of excitation is constant; that the normal component of energy of the excited electron is equal to the work function of the metal and hence is constant; and that the initial unexcited energy of the electron is large in comparison to the energy of the quantum.

The curves for the three cases derived in this paper are plotted in Figure IV using a value σ =-32.2, while a series of three curves for the spherical case are plotted in Figure V.

Dr. Houston has suggested that the orbital motions of the electrons in the space outside of the electrodes may produce appreciable deviations from the ideal case already treated. Accordingly the following analysis is given for the spherical case.

Let the electron be emitted from the cathode with a velocity v in an arbitrary direction with respect to the lines of force. Assume the potential energy to be zero. Let the velocity at aphelion be u. Since here the velocity is entirely normal,

$$u = r_a\dot{\theta}_a$$

Then, since the energy is conserved,

$$\frac{1}{2} mv^2 = \frac{1}{2} mu^2 = Ve$$

where V is the potential at aphelion. Applying the condition of conservation of angular momentum, the following equation results;

$$\frac{1}{2} mv^2 = \frac{1}{2} m\left(\frac{r_a^4}{r_a^2}\right)\dot{\theta}_a^2 + Ve = \frac{1}{2} m \frac{r_c^2}{r_a^2}(\eta^2+\xi^2) + Ve \qquad (14)$$

where r_c is the radius of the cathode and r_a is the aphelion distance. The normal velocity at the cathode is given by

$$r_c \dot{\theta}_c = \sqrt{\eta^2+\xi^2}$$

The external cathode velocity of the electron, in terms of the internal, is given by;

$$v = \sqrt{\xi^2+\eta^2+\zeta^2+\frac{2(hv-W_a)}{m}}$$

Substituting this into equation (14) and collecting terms, there results;

$$r^2 = \frac{r_0^2}{1-P\sin^2\theta} \qquad (15)$$

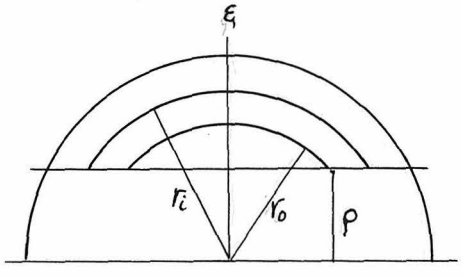

Fig VI

where $P = \left(\frac{r_c}{r_a}\right)^2$ and r, r_0 have their former meanings. Referring to a velocity-space diagram, Fig. VI, it is seen that the available electrons are now limited by a

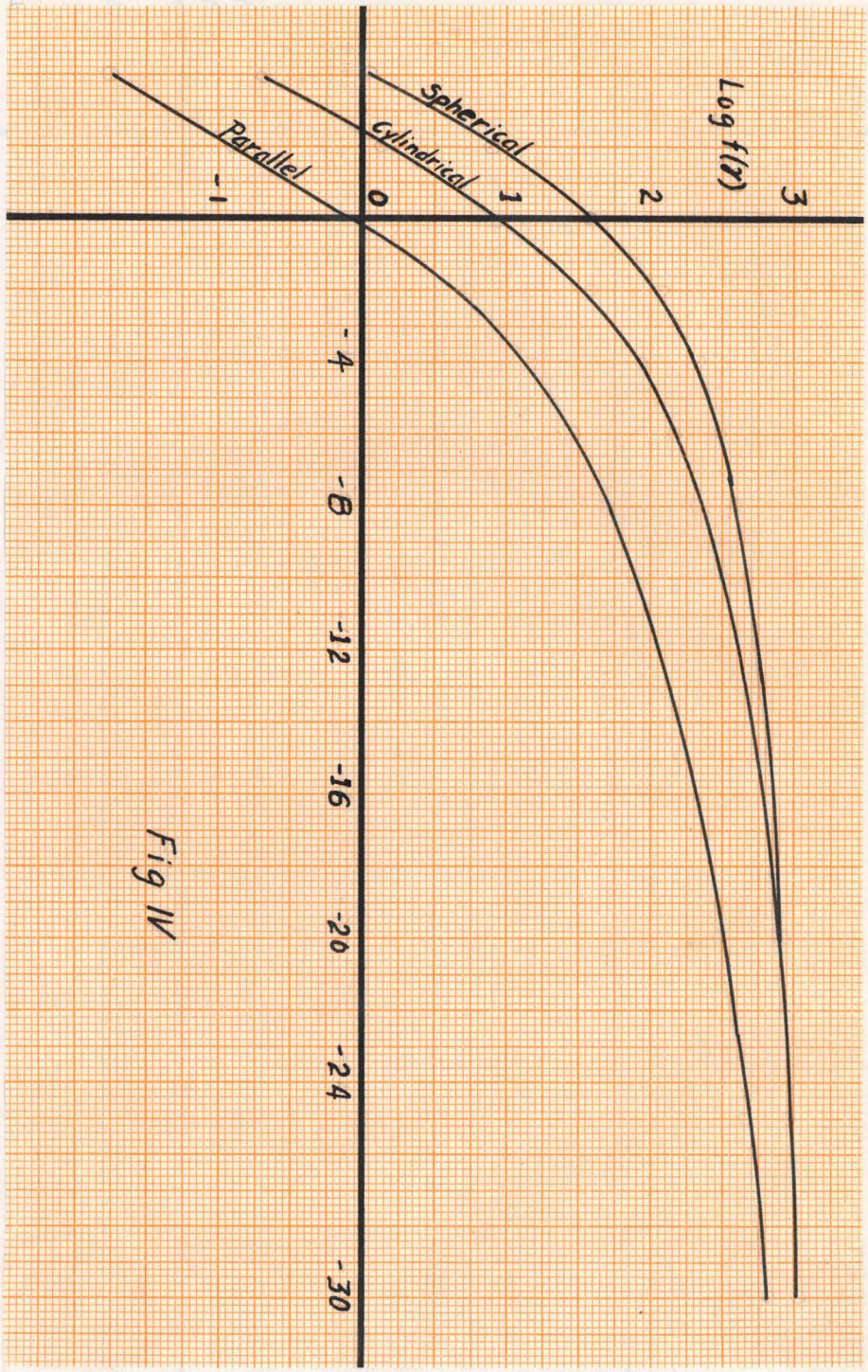
Log f(x)
3
2
1
0
-1
Spherical
Cylindrical
Parallel
-4
-8
-12
-16
-20
-24
-30

Fig IV

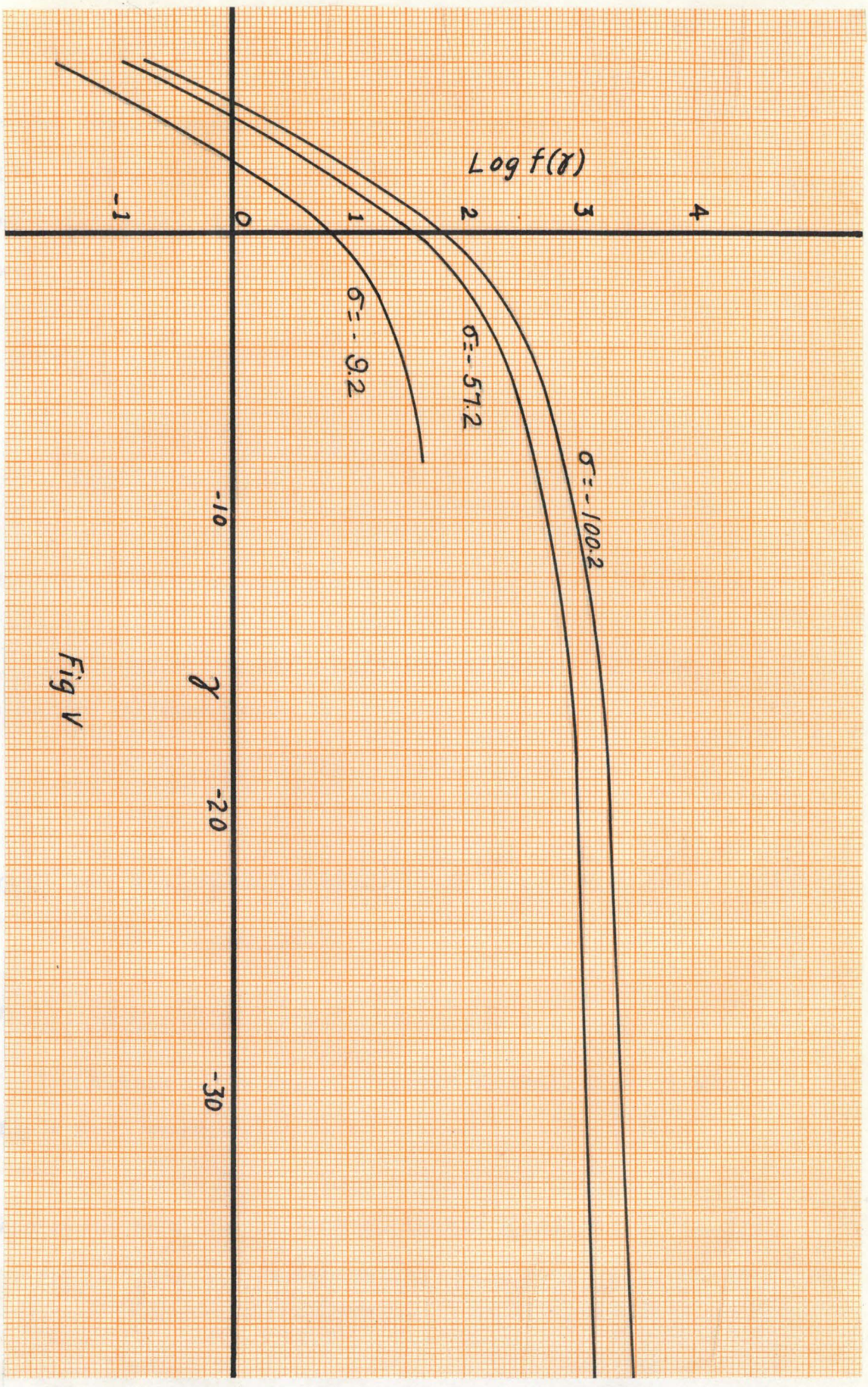

Fig V

spheroidal surface, given by equation 15, whose minor axis r_o is along ξ . Let the intersection of this spheroid with the plane be designated by r_1. Then the equation for the current may be written:

$$i = B\int_0^{2\pi}\int_0^{\cos^{-1}\frac{\rho}{r}}\int_{r_1}^{\infty}\frac{r^3\sin\theta\cos\theta\,dr\,d\theta\,d\phi}{Ae^{\frac{mr^2}{2kT}}+1}$$

$$+ B\int_0^{2\pi}\int_0^{\sin^{-1}\sqrt{\frac{r^2-r_0^2}{r^2}}}\int_{r_0}^{r_1}\frac{r^3\sin\theta\cos\theta\,dr\,d\theta\,d\phi}{Ae^{\frac{mr^2}{2kT}}+1}$$

Upon carrying out the integration and collecting terms, there results the equations:

Range I $\quad \sigma \le \gamma \le \frac{\gamma - P\sigma}{1-P}$

$$i = 2\pi B\left(\frac{kT}{m}\right)^2\left[\frac{\gamma^2}{2(1-P)} - \frac{P}{1-P}\frac{\sigma^2}{2} + \frac{\pi^2}{6} + \frac{\gamma-\sigma}{1-P}\log\left(e^{-\gamma}+1\right) + \left(e^{\frac{\gamma-P\sigma}{1-P}} - \frac{1}{2^2}e^{\frac{2(\gamma-P\sigma)}{1-P}} + \cdots\right)\right] \tag{16}$$

Range III $\quad 0 \le \gamma \le \infty$

$$i = 2\pi B\left(\frac{kT}{m}\right)^2\left[\frac{\gamma-\sigma}{1-P}\log\left(e^{-\gamma}+1\right) - \left(e^{-\frac{\gamma-P\sigma}{1-P}} - \frac{1}{2^2}e^{-2\frac{\gamma-P\sigma}{1-P}} + \cdots\right)\right] \tag{17}$$

The expression for range II was not derived, since it holds for only a short range.

It may be seen by inspection of equations (16) and (17) that as P approaches zero, the expressions for the current become identical

with equations (9) and (10) for the spherical case, while for large values of P, r_i approaches r_o and the second integral above vanishes, leaving the plane-parallel case.

In the experimental set-up used in testing these equations the value of P was about 0.05, so that the electron orbits could produce no appreciable effect.

Apparatus.

A. Photoelectric Cell.

The most important part of the apparatus necessary for carrying on photoelectric measurements is the cell itself. The characteristics of this cell differ radically from those of commercial cells, hence a suitable design must be developed. The characteristics needed are: -

a) High electrical insulation

b) Photoelectric insensitivity of anode

c) Moderate sensitivity of cathode

d) Stability of cathode

e) Reproducibility of readings

f) Electric field of simple symmetry character.

The condition a) is easily fulfilled by having a long insulating path between cathode and anode; b) by using as anode a metal having a high work function and taking care that none of the activating material used on the cathode reaches it; c) by sensitizing the cathode with a thin

layer of one of the alkali metals; d) by using as cathode a metal which does not react with nor dissolve the alkali, and by insuring a high vacuum; e) by so arranging the electrodes that no stray electrons may lodge on the surfaces of the insulators; and f) by using a cell having plane parallel, cylindrical or spherical symmetry.

A number of cells were built and discarded because of failure to meet one or more of these conditions. The one finally adopted is shown in Figure VII. The inner surface of a 300 cc. florence flask was made conducting by means of a thin film of platinum, deposited by evaporation. A tungsten wire, sealed through the glass, permitted contact to be made with the outside. This formed the cathode of the cell. A quartz window W was sealed onto the side of the tube, serving to admit the light. A long tube T attached to the top of the flask served as insulation between the electrodes and supported the cathode C. This cathode consisted of a small iron rod terminating in a tungsten spiral coated with a moderately thin layer of sodium. The side tube S, connected with a sodium reservoir Na, was provided for the purpose of applying sodium to the cathode in a part of the apparatus remote from the anode, A. The tube at the lower part of the flask permitted attachment to a conventional vacuum system.

This cell, which was originally designed for the work on the Marx effect, was found to fulfill admirably all the conditions except f). An inspection of the diagram shows the electric field symmetry of the upper half of the flask to be approximately cylindrical, and

the lower half spherical. This fact escaped notice until after all data were taken, but is sufficient to invalidate any conclusions drawn from comparison of theory and experiment.

B. Electrical System.

The requirements that must be met by the electrical system are: -

a) Measurement of currents in the range 10^{-12} to 10^{-16} amperes.

b) A means of varying the potential difference between cathode and anode in small steps.

c) Accurate measurement of potential differences

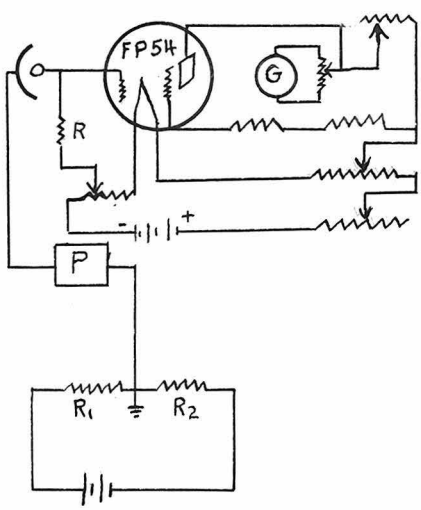

Fig VIII

The cathode of the cell was connected with two parallel circuits, one branch going to the grid of a General Electric F. P. 54 pliotron and the other to ground through a resistance R_1 of value 2.6×10^{10} ohms, as shown in Figure VIII. The pliotron was used in a DuBridge[3] circuit with a Leeds and Northrup type H. S. 2285c galvanometer for measuring the variations in

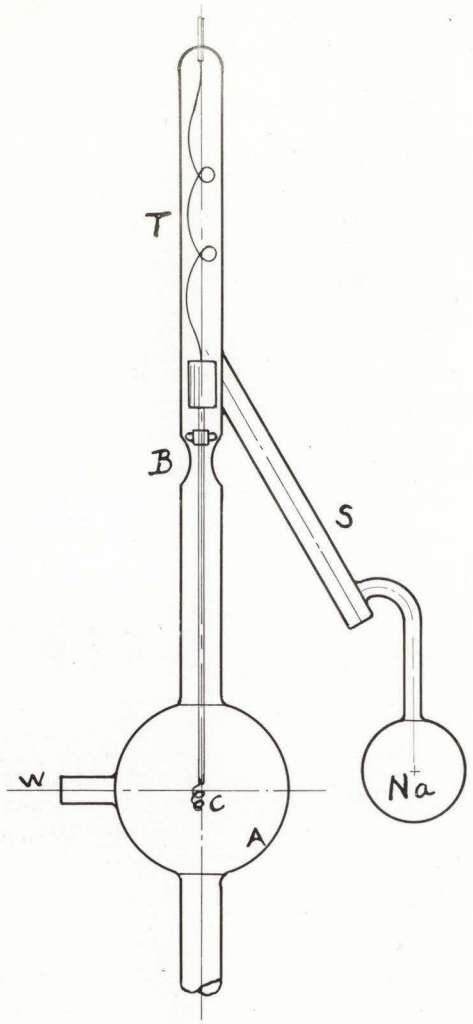

Fig VII

the plate current caused by the photoelectric currents. Application of known potentials to the grid gave very nearly linear response on the galvanometer with a maximum sensitivity of 1.8×10^{-4} volts/cm. on a scale 3 meters distant. The zero point showed a small drift of approximately 8×10^{-4} cm/sec.

Voltages were applied to the anode by means of a storage battery V and the resistance dividers R and R_2, which were 10,000 ohm dial resistance boxes. The values of the voltages were determined to 0.001 volt by means of the Leeds and Northrup type K potentiometer P.

All electrical parts were enclosed in grounded metal cases with connecting leads carried in woven cable. The grid lead was made as short as possible, being about 10 cm in length and further enclosed in an air-tight container which could be evacuated. However, evacuation produced no measurable improvement, so was not used.

C. Light System.

The source of light was a Cooper Hewitt quartz 220 volt horizontal mercury arc connected with a voltage-controlled D. C. generator, supplying 220 volts. The circuit also contained a series resistance and inductance of such values that the voltage across the arc was maintained at 130 to 160 volts, the particular value being maintained constant during an entire run. It was not found possible to maintain the current steady, fluctuations occurring through a maximum range of 0.5 amperes, and being caused by return of condensed mercury to the

anode. However it was noticed that the photoelectric current fluctuated in phase with the arc current, so the convention was adopted of taking all photocell readings at the same arc current reading. In this manner photocell currents could be duplicated.

Light from the arc A of Figure IX passed through the slit S of a Hilger monochromatic illuminator M and emerged as a monochromatic beam at S_2 from which it passed through a shutter and filter cell at B. A quartz lens L focussed the beam on the cathode of the photocell C.

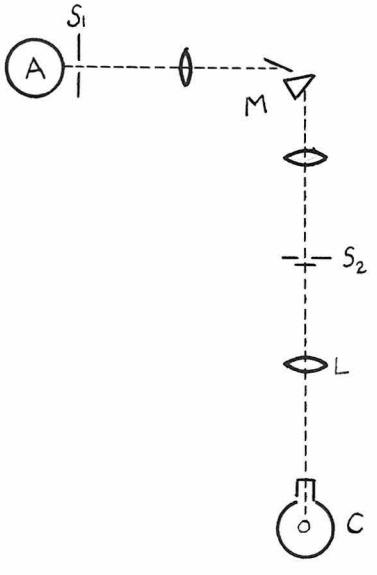

Fig IX

In the region of long waves, the dispersion of the illuminator was not sufficient to give the desired separation of lines, so filters were used as shown in Table I.

Table I

	Filter				Transmission of	
5770	Wratten 22				5461	trace
5461	$CuCl_2$	.398N	$CaCl_2$	4.041N	4358	trace
4358	$CuCl_2$	.398N	$CaCl_2$	0.812N	4046	3
4046	$CuCl_2$	.398N	$CaCl_2$	0.271N	3650	2
3650	$CuCl_2$	....	$CaCl_2$	....	3126	1
3341	Cobalt glass			.....		

Experimental Proceedure and Data.

The photocell, with freshly distilled sodium in the reservoir, was mounted on the pumps, evacuated to a pressure of about 10^{-7} mm of mercury, as shown by an ionization gauge, and baked out for several hours at a temperature of 490° C. During this time the sodium in the reservoir was outgassed by maintaining it at its melting point for some minutes. After completion of this baking, the cathode was moved magnetically to the distilling chamber S of Figure VII where it was brought to a bright red heat by means of an induction furnace. A coating of sodium was then distilled up from the reservoir and deposited on the tungsten spiral. This coat was of sufficient thickness to produce a barely perceptible whitening of the spiral. The cathode was then returned to the center of the flask, the beam of light from the monochromater adjusted to fall on the activated spiral, shields put in place and electrical circuits completed.

The sodium surfaces were not stable for the first few hours after application, showing a rising sensitivity which became constant after about 12 hours, when they showed a very satisfactory reproducibility for a period of about a week after which the sensitivity became lessened to such an extent that they were replaced. It is worthy of remark that a previous cathode of copper, and one of platinum plated copper both showed this same instability in a much accelerated manner, leading to the belief that some action occurred between the sodium and the metal of the cathode. This same effect was mentioned

by Brady[4] in connection with experiments conducted at the University of California.

The routine of collecting the data was carried out in the following manner: - The arc was started with the monochromator set on an appropriate line of the spectrum and while it was warming up, the sensitivity of the pliotron circuit was measured by applying known potentials to the grid and noting the corresponding galvanometer deflections. A positive potential, somewhat less than that necessary to give saturation currents, was applied to the anode of the photocell and the galvanometer reading was noted with the shutter closed, opened and again closed. These readings yielded a value of the photocurrent approximately corrected for zero drift. The anode voltage was measured by the potentiometer. Resistances R and R_2 were changed, keeping the sum equal to 10,000 ohms and the readings repeated. This proceedure was followed, changing the anode voltage in steps of about 0.05 until the photocurrents were reduced to values of approximately 10^{-15} amperes. The anode voltages, which were referred to ground, had still to be corrected for the rise of cathode potential before obtaining the true potential difference between anode and cathode. This rise of cathode potential was obtained from the sensitivity calibration curves.

Three sets of data were taken, of which that taken on the date of 7/18 using the mercury 4358 line and given in Table III is a representative sample.

Table III

Sens	D_o	D_L	D_o'	R_1	V_{anode}	I_{Arc}	V_{Arc}	$\bar{D}$	$V_{cathode}$	V	Ve/kt	I/I_o	log I/I_o
0.1	10.1	52.1	10.2	5300	1.949	3.0	134	41.9	0.105	1.844	71.5	1.000	0.00
	10.1	48.9	10.1	5200	1.912	3.0	132	38.8	0.097	1.815	70.4	0.992	0.036
	10.1	45.6	10.1	5100	1.875	3.0	134	35.5	0.088	1.786	69.3	0.840	0.076
	10.1	42.4	10.2	5000	1.838	3.0	133	32.2	0.080	1.758	68.1	0.758	0.120
	10.1	38.9	10.2	4900	1.801	3.0	133	28.7	0.071	1.730	67.1	0.675	0.170
	10.1	35.7	10.2	4800	1.764	3.0	134	25.5	0.063	1.701	66.0	0.600	0.222
	10.2	32.3	10.2	4700	1.728	3.0	133	22.1	0.055	1.674	65.1	0.519	0.285
	10.2	29.4	10.2	4600	1.692	3.0	132	19.2	0.047	1.645	63.8	0.450	0.347
	10.2	26.2	10.3	4500	1.656	3.0	132	16.0	0.039	1.617	62.7	0.372	0.430
	10.2	23.2	10.2	4400	1.620	3.0	132	13.0	0.032	1.588	61.6	0.301	0.522
	10.2	20.4	10.2	4300	1.584	3.0	134	10.2	0.025	1.559	60.5	0.236	0.626
	10.2	17.8	10.2	4200	1.548	3.0	134	7.6	0.018	1.530	59.3	0.176	0.756

Table III

(continued)

Sens	D_o	D_L	D_o'	R_1	V_{Anode}	I_{Arc}	V_{Arc}	$\bar{D}$	$V_{cathode}$	V	Ve/kt	I/I_o	log I/I_o
1.0	15.7	86.5	15.9	4100	1.582	3.0	134	70.7	0.013	1.500	58.2	0.121	0.917
	15.8	61.6	16.1	4000	1.477	3.0	132	45.6	0.008	1.469	57.0	0.078	1.109
	16.0	41.8	16.2	3900	1.441	3.0	133	25.7	0.005	1.436	55.7	0.0442	1.355
	16.2	29.4	16.4	3800	1.405	3.0	134	13.1	0.002	1.403	54.5	0.0225	1.648
	16.4	22.4	16.6	3700	1.370	3.0	132	6.9	0.001	1.369	53.1	0.0119	1.924
	16.6	19.2	16.8	3600	1.335	3.0	134	2.5	0.000	1.334	51.8	0.99447	2.350

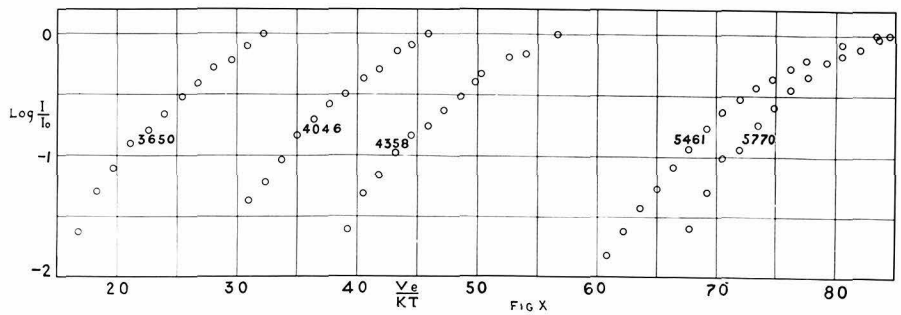
0
-1
-2
Log I/I₀
3650
4046
4358
5461
5770
20
30
40
Ve/KT
50
60
70
80

FIG X

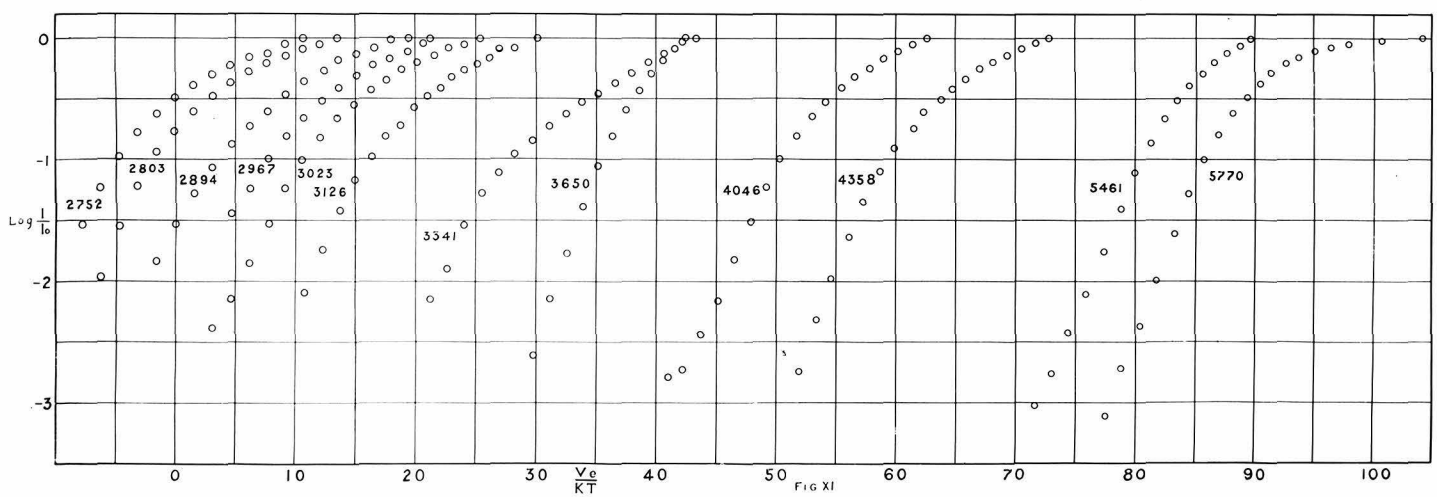
0
-1
-2
-3
Log I/I₀
2752
2803
2894
2967
3023
3126
3341
3650
4046
4358
5461
5770
0
10
20
30
Ve/KT
40
50
60
70
80
90
100

FIG XI

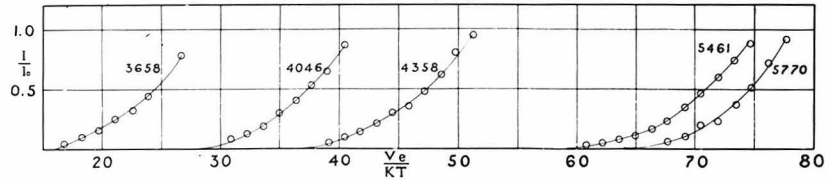

Fig XIII

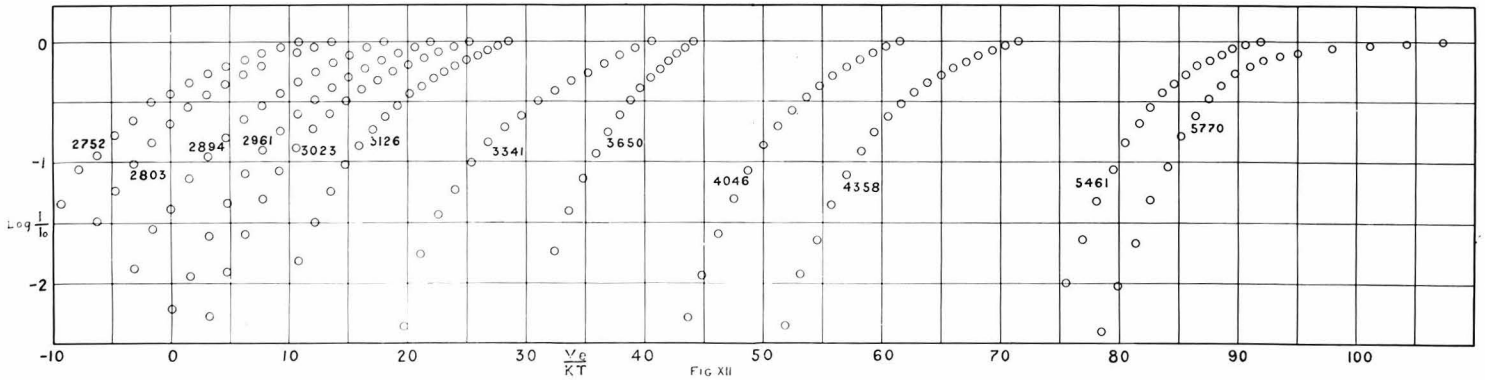

Fig XII

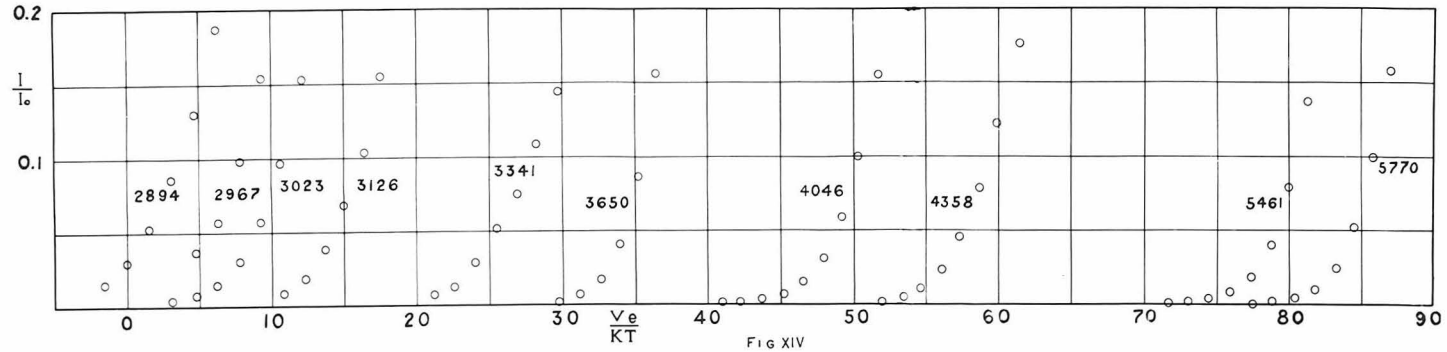

FIG XIV

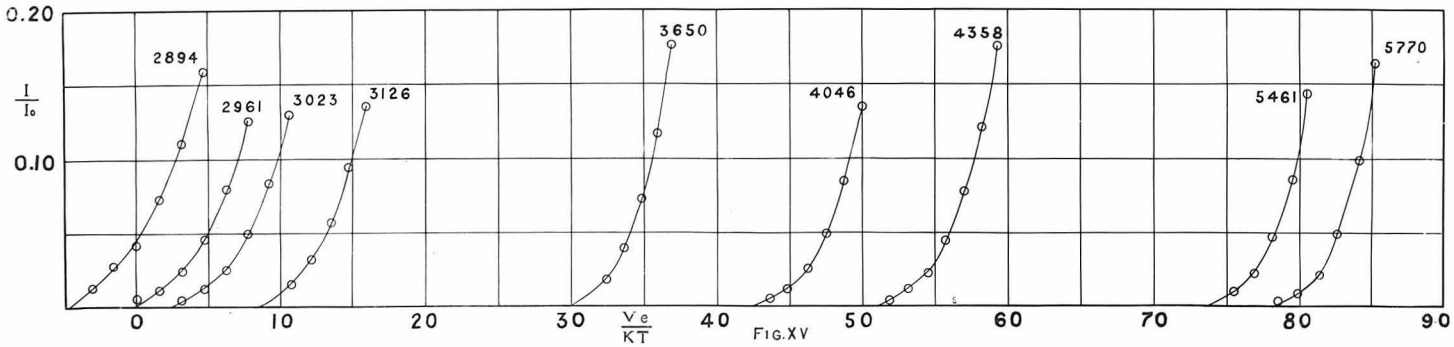

FIG.XV

Curves from the three sets of data are shown in Figures X, XI, and XII, where log I/I is plotted against Ve/kT, the value of 300° A being taken for the temperature. While these curves are seen to have the same general shape of the theoretical ones shown in Figures IV and V, all attempts to superimpose one set over the other have failed. From the symmetry characteristics of the tube, it might be expected that the experimental curves would lie between the spherical and cylindrical cases. Actually they correspond more closely with the plane parallel case. When an attempt was made to determine h by applying this case to the data of 7/14 and 7/18, the value obtained was

$$h = (6.65 \pm 0.02) \times 10^{-27}$$

This value agrees with a reported determination of DuBridge[5], using a similar method, in being 2% above the accepted value.

Figures XIII, XIV and XV show the current plotted against Ve/kT for the three sets of data. The curves of Figure XIV clearly show the difficulties involved in the extrapolation method of determining stopping potentials. In this set the small currents from strong spectral lines represent points far out on the tails of the curves, while those from the weak lines are too far up on the curves to give reliable extrapolations. The sets shown in Figures XIII and XIV chance to be better adapted to this treatment if the three weak lines 2752, 2803 and 3341 be discarded from the latter set. The extrapolations then give the following values;

Table IV

	Ve/kT	
5770	63.8	78.1
5461	59.2	73.5
4358	37.5	50.9
4046	28.2	42.4
3650	15.9	29.8
3126	----	8.1
3022	----	2.3
2967	----	- 0.2
2894	----	- 4.8

Solution of the Einstein equation for h by the method of least squares yields;

$$h = (6.518 \pm 0.035) \times 10^{-27}$$

for the set of five lines, and

$$h = (6.540 \pm 0.012) \times 10^{-27}$$

for the set of nine lines, while Birge's[6] value is

$$h = (6.547 \pm 0.008) \times 10^{-27}$$

Conclusion

The method, outlined in the preceeding pages, of determining the photoelectric stopping potentials associated with the various frequencies of exciting light by means of theoretical curves which permit the use of currents throughout the entire range of voltages rather than a few at the lower ends of the curves is one which gives

great promise of improving the accuracy of the value of Planck's constant. The universal character of the curves for the plane parallel case makes this type of electrodes desirable, although the greater currents arising from the other two symmetry types is also a factor which should be considered.

The failure, in the present work, to obtain values of h more nearly in accord with the accepted value may be due to one of the following reasons: -

(1) Error in accepted value

(2) Invalidity of theoretical assumptions

(3) Systematic error in data

(4) Incorrect application of theory to experiment

The first reason hardly seems plausible in view of the careful analysis by Birge[6] of the consistency of fundamental constants.

The theoretical assumptions will now be discussed in somewhat more detail than previously.

a) The Fermi distribution of electron momenta.

This distribution applies to an assemblage of electrons in a quantized system and, consequently, the electrons must possess potential energy. Just how far one is justified in neglecting this potential energy is not known, nor is it clear how this energy is to be included in the computations. However, it seems probable that a good approximation should result through the neglect of it in the case of frequencies near the threshold. Since the experimental curve for the 5770

line fits the theory no better than others, it is doubtful if this assumption is responsible for the discrepancy betwen theory and experiment.

b) Entire quantum absorbed by one electron.

This follows from the wave mechanical treatments of the interaction between light and electrons given by Wentzel[7], Tamm and Schubin[8], and Mitchell[9].

c) Energy of absorbed quantum appears as increased motion normal to surface of metal.

There seems to be no direct experimental or theoretical justification for this assumption, but it will be retained in the absence of knowledge regarding the direction of emission of this energy.

d) Probability of absorption of quantum is proportional to normal component of velocity.

This also follows from the wave mechanical treatment of the problem.

e) Probability of escape of electron from surface is unity if energy is greater than W_a and is zero if energy is less than W_a.

For metal surfaces of thickness greater than monomolecular layers, a simple potential wall may be assumed to exist between metal and outer space which, according to wave mechanical treatments, will give the assumed transmission probability.

In the light of present knowledge there seems to be no reason for changing any of these assumptions and until all other causes of

discrepancy between theory and experiment have been eliminated, they must stand.

Any systematic error in the data might be expected to cause erratic values of h when computed by the extrapolation method, but it is seen that the value obtained from the five lines is within 1/2 of 1% of the Birge value which is as close as can be expected from the limited range. The value using the more extended range comes within 1/10 of 1% of Birge. The data of 7/14, while not adapted to the extrapolation method, nevertheless are consistent with those of 7/18, as shown by comparison with the theoretical curves, one set giving;

$$h = 6.67 \pm 0.02$$

and the other

$$h = 6.64 \pm 0.02$$

Because of these results, it seems safe to rule out the possibility of consistent error in the data.

The only remaining source of difficulty lies in the incorrect application of the theory, and this is by far the most serious. As previously pointed out, the electric field in the experimental cell does not correspond with any of the theoretical cases. While this is the most probable cause of failure, there still remains the fact to be explained that DuBridge got similar results when using a tube of much better symmetry characteristics than the one used in this work.

It also appears that DuBridge's data fit his theoretical curves only in the neighborhood of $\gamma = 0$, in which region the data of this experiment fit with fair success. But if the theory is to prove of value in quantitative determinations, the fit must be much better than it is at present.

Until further work has been carried out, eliminating some of the objectionable features outlined above, no definite conclusions can be drawn regarding the application of theoretical curves to the problem of determining stopping potentials.

The Marx Effect

In 1929, E. Marx[10], at Leipsig, announced a new photoelectric effect which was later experimentally verified by Marx and Meyer[11]. Marx showed that the stopping potential associated with a given frequency of incident light was decreased upon simultaneous illumination with a second light of lower frequency, the amount of the decrease being given by

$$R = const \frac{n_2}{n_1 + n_2 b} (\nu - \nu_1) \frac{\nu_1}{\nu_2} \frac{h}{e} \qquad (1)$$

where n_1 is the intensity of the light of frequency ν_1, n_2 that of ν_2, b is a constant to be determined experimentally; h is Planck's constant and e the charge on the electron.

Since this effect is not one to be expected on the basis of

ordinary views of photoelectricity, an attempt was made to verify the relation.

Discussion of Theory

For a complete account of the Marx theory, the reader is referred to the original papers. However, an outline of the proof will be given here, together with a discussion of the most controversial points.

The Einstein equation

$$h\nu = Ve - (b + A) \tag{2}$$

forms the starting point of the discussion, where A is a term added to the ordinary work function b and arises from the work done by the electron in traversing an external and internal space-charge. It is shown that A will be given by the expression

$$A = 4\pi e \int_{-\infty}^{+\infty} dx \int_{-\infty}^{x} \rho dx \tag{3}$$

where x is the distance from the illuminated electrode and ρ is the space-charge. To find the way in which ρ varies with x, Marx makes use of an empirical distribution function due to Ramsauer[12] and holding for electrons emitted by monochromatic light

$$y = a'\varepsilon^4 \left(e^{2\varepsilon^2} - 1\right)^{-1} \tag{4}$$

where y is the number of electrons having energy of emission ε.

If now the emitting electrode be one plate of a charged condenser and if the electrons be subjected to a retarding field they will be turned back after traversing a potential difference V given by

$$Ve = \mathcal{E}$$

Furthermore if the plates of the condenser be plane

$$V = EX$$

and

$$EeX = \mathcal{E}$$

or

$$y = a'(Eex)^4\left[e^{2(Eex)^2} - 1\right]^{-1} \qquad (5)$$

which gives the number of electrons having maximum range X, or the number having rest points at X. The assumption is now made that "the distribution of the rest-points along the X-axis must correspond with the distribution of space-charge along the distance axis."

It is seen that the expression (5) will have a maximum at some point V = K along the voltage axis. If V_i represents the stopping potential for the frequency ν_i then

$$\overline{C}_o V_i = K \qquad (6)$$

where "$\overline{C}_o$ is a universal constant for all frequencies". The expression for ρ is now given as

$$\rho = a\left(\frac{x}{k}\right)^4\left[e^{2\frac{x^2}{k^2}} - 1\right]^{-1} \qquad (7)$$

where a has the dimensions of space charge ($a < 0$).

It is assumed that electrons, acted upon by the light, but not yet freed from the metal, will have a distribution along the negative x-axis of the same form as (7), but with different constants a' and k'. Inserting these values into equation (3), and carrying out the integration, there results as the work done by an electron in traversing the space-charge, the expression

$$A = 4\pi e C_o a k(k + k') \qquad (8)$$

The next step in the development of the theory consists in showing that the magnitude of the space-charge is independent of the intensity of illumination. For this purpose, there is introduced a fictitious "influence-capacity", C, which is defined as the capacity between the illuminated electrode and a parallel plane passing through the point at which the maximum electron density occurs in the space between electrodes. Since this position of maximum has already been shown to be independent of the frequency and intensity of the incident light, it follows that C is constant. If, now, the electrode be illuminated at time $t = 0$, the charge on the fictitious condenser-plate at time t will be given by

$$\bar{c}_o C V_t = Q_t \qquad (9)$$

The increase in charge is then given by

$$\frac{d}{dt}(\bar{c}_o C V_t) = ne - \beta n C \bar{c}_o V_t \qquad (10)$$

where n is the number of electrons emitted per sec.; V_t is the potential of the electrode at time t; $\bar{c}_o$ is, as before, a proportionality constant relating k and V; and β is a constant depending on the rate of return of electrons to the electrode. Equation (10), upon integration, yields the result:

$$V_t = V_g(1 - e^{-\beta n t}) \qquad (11)$$

where $$V_g = \frac{e}{\beta C \bar{c}_o}$$

When t becomes infinite V_t approaches a constant value V_g which is independent of n, hence the potential due to the space-charge and also the space-charge itself is independent of the intensity of illumination.

It is seen that this surprising result is due to the assumption that the rate of return of electrons from the space-charge is proportional to the rate of emission. There is no attempt made to justify this and indeed there seems to be no justification for it. The more reasonable way of writing equation (9) is

$$\frac{dQ}{dt} = ne - \beta Q$$

which leads to

$$Q = \frac{ne}{\beta}(1 - e^{-\beta t})$$

The above objections are sufficient to show that the theory of the Marx effect is not entirely reliable, so no further time will be spent on this phase of the question but attention will now be turned to the experimental test.

Apparatus

The photoelectric cell used in this experiment was the one previously described and pictured in Fig. VII. The electrical circuits were the same with the exception that a Compton electrometer was used in place of the General Electric pliotron.

The light system was somewhat more complicated in this investigation since stray light of frequencies both above and below the ones in use had to be excluded. For this purpose two Hilger illuminators were utilized as shown in Fig. XVI. Light from mercury quartz arc A passed through lens L_1 into illuminator M_1 where it was split up into its monochromatic beams. After leaving M_1, it passed through lens L_2 and

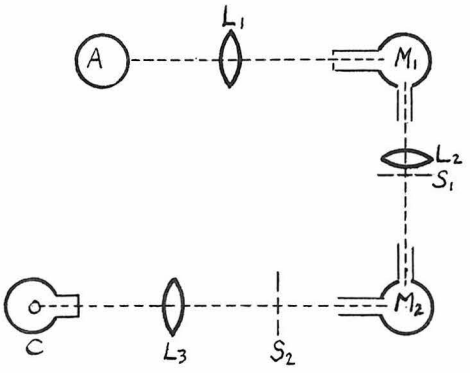

Fig XVI

slit S_1, lying close behind L_2. This slit allowed the passage of two beams of frequencies ν_1 and ν_2. Illuminator M_2 further resolved these beams and slit S_2 removed stray light passed by M_1. Lens L_3 then focussed the light on the cathode of the photocell C.

- Data -

A preliminary test of the Marx effect was made using a Burt photoelectric cell, illuminated with while light. The anode of the cell was grounded and the cathode was connected to one pair of quadrants of the Compton electrometer. With this arrangement the cathode acquired the stopping potential V as shown by the deflection of the electrometer. Upon insertion of a cobalt glass filter into the path of the light the deflection increased showing the new stopping potential V_i to be greater than V. This, qualitatively, was the effect discussed by Marx.

The previously described apparatus was then set up and voltage-current curves were taken for the lines 5461 alone, 4358 alone and the two together. The curves so obtained are shown in Fig. XVII. An inspection of these curves shows that there is no indication of a change in the 4358 stopping potential due to the presence of the 5461 line.

Conclusion

In view of the close agreement between the curves $I(\lambda_1+\lambda_2)$ and $I(\lambda_1)+I(\lambda_2)$ in the threshold region where Marx prdicts a

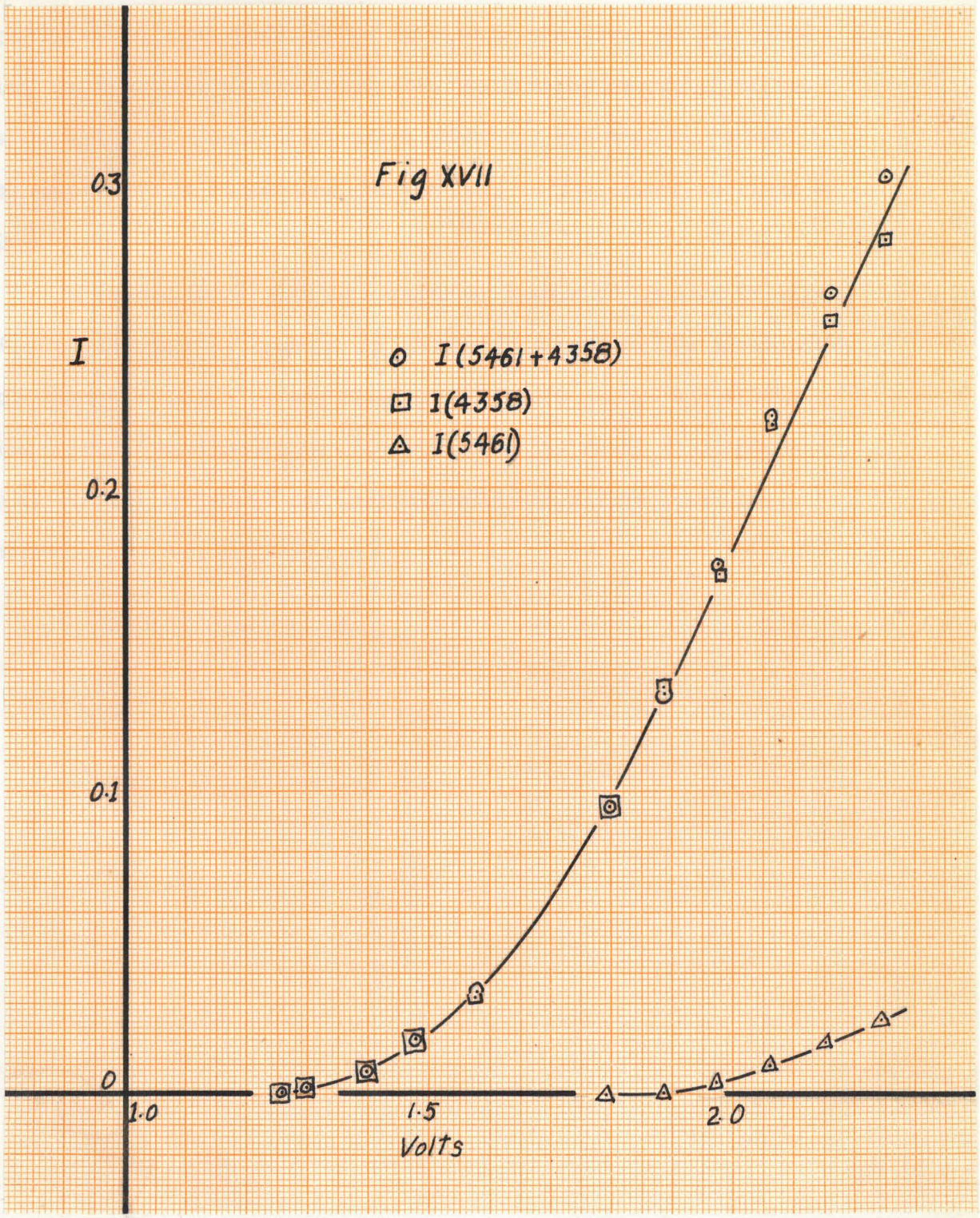
Fig XVII
I
0·3
0·2
0·1
0
I (5461 + 4358)
I (4358)
I (5461)
1·0
1·5
2·0
Volts

large variation, and furthermore, in view of the flaws in the theoretical analysis, it is concluded that the new photoelectric effect does not exist in a well constructed photocell and that the effect which does exist in commercial cells is due to the causes ascribed by Olpin[13].

In conclusion I wish to express my thanks to Doctors William V. Houston and Paul S. Epstein for their assistance in the development of the theory outlined in the first part of this paper; and to the entire staff of Norman Bridge Laboratory for the ready willingness with which they discussed the many experimental difficulties encountered.

References

1) Fowler, Phys. Rev., 38, 45; 1931.

2) DuBridge, Phys. Rev., 43, 727; 1933.

3) DuBridge, R.S.I., 4, 532; 1933.

4) Brady, Phys. Rev., 41, 613; 1932.

5) DuBridge,

6) Birge, Phys. Rev., 40, 228; 1932.

7) Wentzel, Sommerfeld Festschrift, 79; 1928.

8) Tamm and Schubin, Zeit. f. Physik, 68, 97; 1931.

9) Mitchell, Proc. Roy. Soc., 146, 442; 1934.

10) Marx, Naturwissenschaften, 17, 806; 1929.

11) Marx and Meyer, Phys. Ztschr., 32, 153; 1931.
Ann. der Phys., 9, 787; 1931.

12) Ramsauer, Ann. der Phys., 45, 1121; 1914.

13) Olpin, Phys. Rev., 35, 112; 1930.